CHEMISTRY
A EUROPEAN JOURNAL

DOI: 10.1002/chem.200600733

Activation of the Disulfide Bond and Chalcogen–Chalcogen Interactions: An Experimental (FTICR) and Computational Study

M'Hamed Esseffar,*[a] Rebeca Herrero,[b] Esther Quintanilla,[b] Juan Z. Dávalos,[b] Pilar Jiménez,[b] José-Luis M. Abboud,*[b] Manuel Yáñez,[c] and Otilia Mó[c]

Abstract: Dimethyldisulfide (**I**) is the simplest model of the biologically relevant family of disubstituted disulfides. The experimental study of its gas-phase protonation has provided, we believe for the first time, a precise value of its gas-phase basicity. This value agrees within 1 kJ mol^{-1} with the results of G3 calculations. Also obtained for the first time was the reaction rate constant for the bimolecular reaction between **I** and its protonated form, $\mathbf{I}H^+$, to yield methanethiol and a dimethyldithiosulfonium ion. This constant is of the order of magnitude of the collision limit. A computational mechanistic study based on the energetic profile of the reaction, completed with Fukui's and Bader's treatments of the reactants and transition states fully rationalizes the regioselectivity of the reaction as well as the existence of a shallow, flat Gibbs energy surface for the reaction. The mechanistic relevance of the chalcogen–chalcogen interaction and the C–H···S bonds has been demonstrated.

Keywords: basicity · bond activation · chalcogen–chalcogen interactions · FTICR · gas-phase reactions · MP2 calculations

Introduction

It has been known for some time that the disulfide group (S–S) is an important constituent of many proteins.[1–3] Quite recently, the study of the mechanism of the action of proton pump inhibitors (PPIs) has revealed that these compounds are prodrugs that inhibit the acid-secreting gastric (H^+,K^+)-ATPase by acidic activation to reactive thiophilic species that form disulfide bonds with one or more cysteines accessible from the exoplasmic surface of the enzyme.[4] Irrespective of the potential relevance of the disulfide bond in protein folding,[3] it is clear that its activation is relevant from the fundamental and applied points of view.

Initial experimental studies of the disulfide exchange reaction [Eq. (1)] in solution,

$$R^1SSR^1 + R^2SSR^2 \rightarrow 2R^1SSR^2 \quad (1)$$

led us to consider the protonated form of these compounds, $(RSSR)H^+$ as a key reactive species in this reaction (the overall process in solution might well be a complex one).[5]

In a classical study by means of ion cyclotron resonance (ICR)[6] Caserio, Kim and Bonicamp[7] carefully examined the gas-phase protonation of dimethyldisulfide, CH_3SSCH_3 (**I**), by protonated reference bases, $B_{ref}H^+$, see Equation (2).

$$\mathbf{I}(g) + B_{ref}H^+(g) \rightarrow \mathbf{I}H^+(g) + B_{ref}(g) \quad (2)$$

These authors found that $\mathbf{I}H^+$ ($m/z = 95$) reacts extremely fast with the neutral **I** present in the ICR cell to yield dimethyldithiosulfonium ion ($\mathbf{II}^+$) ($m/z = 141$), see Equation (3).

$$(CH_3{-}SH{-}S{-}CH_3)^+ + CH_3{-}S{-}S{-}CH_3(g) \rightarrow (CH_3{-}S(SCH_3){-}S{-}CH_3)^+(g) + CH_3SH(g) \quad (3)$$

In fact, this reaction proceeded so fast after the formation of $\mathbf{I}H^+$ that they could only give a bracketing estimate of

[a] Prof. Dr. M. Esseffar
Département de Chimie, Faculté des Sciences (Semlalia)
Université Cadi Ayyad, Marrakesh (Morocco)
Fax: (+212) 24437408

[b] M.Sc. R. Herrero, Dr. E. Quintanilla, Dr. J. Z. Dávalos, Dr. P. Jiménez, Prof. Dr. J.-L. M. Abboud
Instituto de Química Física Rocasolano
CSIC. C/Serrano 119, 28006 Madrid (Spain)
Fax: (+34)915855184
E-mail: iqrla78@iqfr.csic.es

[c] Prof. Dr. M. Yáñez, Prof. Dr. O. Mó
Departamento de Química C-9 Universidad Autónoma de Madrid
Canto Blanco, 28049 Madrid (Spain)

Supporting information for this article is available on the WWW under http://www.chemeurj.org/ or from the author.

the gas-phase basicity (GB) of **I**,[8] GB(**I**) = 764–781 kJ mol^{-1}.[9]

To our knowledge, the determination of GB(**I**) has not been attempted again and the mechanism of the reaction in Equation (3) has not yet been established. On account of the relevance of the disulfide bond, we have carried out a systematic experimental study of the reactions in Equations (2) and (3) by using Fourier Transform Ion Cyclotron Resonance spectrometry (FTICR) as well as a computational study of both processes.

Experimental Section

Materials: *n*-Butyl trifluoroacetate was obtained from the reaction between trifluoroacetic anhydride and *n*-butanol. Its final purification stage was a distillation through a Perkin–Elmer adiabatic spinning band annular still (100 theoretical plates). Malononitrile (Fluka) was sublimed twice. All other products were of commercial origin (Aldrich) and of the highest purity available.

Gas-phase studies

The FTICR spectrometer: In this work, use was made of a modified Bruker CMS 47 FTICR mass spectrometer. A detailed description of the original instrument is given in reference [6d]. It has already been used in a number of studies.[10] Some salient features are as follows: the spectrometer is linked to an Omega Data Station (Ion Spec, CA). The high-vacuum is provided by a Varian TURBO V550 turbomolecular pump (550 L s^{-1}). The magnetic field strength of the superconducting magnet is 4.7 T.

Working conditions: Mixtures of **I** and a reference base B_{ref} of known gas-phase basicity were introduced into the high-vacuum section of the instrument. Typical partial pressures were in the range of 1×10^{-8}–5×10^{-7} mbar. The average temperature of the cell was approximately 323 K. The mixture was ionized by electron ionization, using energies in the range of 12–20 eV and ionic fragments of **I** and B_{ref} acted as proton sources (chemical ionization). In all cases, approximately 1×10^{-6} mbar of argon were added. After reaction times of 2–5 s, ions $B_{ref}H^+$ thus formed, were isolated by means of ion-selection techniques and reacted with **I** for times of up to 120 s (depending on the acidity of $B_{ref}H^+$). It was established in all cases that the reactions in Equations (2) and/or (3) were the only observed processes.

The pressures of the neutral species were measured with a Bayard–Alpert ion gauge. Readings were corrected according to the method of Bartmess and Georgiadis,[11] by using for each compound, the polarizabilities, α(ahc) calculated following Miller's method.[12]

Kinetic studies: Elementary processes in Equations (2) and (3) follow second order kinetics. Let k_1 and k_2, respectively, stand for their respective reaction rates. Equations (4) and (5) express this fact:[13]

$$\frac{dP_{\mathrm{BrefH+}}}{dt} = -k_1 P_{\mathrm{BrefH+}} P_{\mathbf{I}} \quad (4)$$

$$\frac{dP_{\mathbf{I}H+}}{dt} = k_1 P_{\mathrm{BrefH+}} P_{\mathbf{I}} - k_2 P_{\mathbf{I}} P_{\mathbf{I}H+} \quad (5)$$

Equations (6)–(8) follow:

$$P_{\mathrm{BrefH+}} = (P_{\mathrm{BrefH+}})_{\mathrm{init}} \exp(-k_1 P_{\mathbf{I}} t) \quad (6)$$

$$P_{\mathbf{I}H+} = (P_{\mathrm{BrefH+}})_{\mathrm{init}} \left[\frac{k_1}{(k_2-k_1)}\right] [\exp(-k_1 P_{\mathbf{I}} t) - \exp(-k_2 P_{\mathbf{I}} t)] \quad (7)$$

$$P_{\mathbf{II}+} = (P_{\mathrm{BrefH+}})_{\mathrm{init}} \left[\frac{1}{(k_2-k_1)}\right] [k_2 \exp(1-k_1 P_{\mathbf{I}} t) - k_1 \exp(1-k_2 P_{\mathbf{I}} t)] \quad (8)$$

Relative intensities of the ion signals are taken as directly proportional to the relative abundances (or partial pressures) of the various ionic species. In this study, the temporal evolution of the relative intensities of ions $B_{ref}H^+$, $\mathbf{I}H^+$, and $\mathbf{II}^+$ was monitored. The temperature of the cell, as determined by a platinum resistor was 323 K.[10c,14]

The ion gauge was calibrated by measuring the rate constant for the reaction in Equation (9)[14]

$$[CH_3OH]^{+\cdot} + CH_3OH \rightarrow CH_3O^{\cdot} + CH_3OH_2^+ \quad (9)$$

and by considering that for this process the rate constant equals $(2.30\pm0.29)\times10^{-9}$ cm^3 molecule^{-1} s^{-1}.[10c]

Under the experimental working conditions, $P_{\mathbf{I}}$ is constant in each experiment and the reaction in Equation (4) is of pseudo first order. From a series of experiments involving different pressures of **I**, $k_1P_{\mathbf{I}}$ values were obtained by using the logarithmic form of Equation (6). From the direct proportionality with $P_{\mathbf{I}}$, they provided values of k_1. They were used to determine k_2 by means of Equations (7) and (8).

Figure 1 is a representative plot of the experimental kinetic information obtained by using ethyl formate, $HCOOC_2H_5$, as B_{ref}. Species $B_{ref}H^+$, $\mathbf{I}H^+$, and $\mathbf{II}^+$ have *m*/*z* values of respectively 75, 95, and 141. The pattern

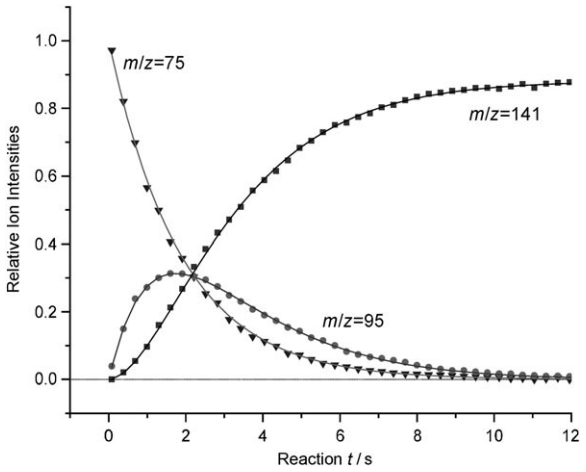

Figure 1. Temporal evolution of the relevant ion intensities. B_{ref} = HCO_2Et. $P_{\mathbf{I}} = 3.3\times10^{-8}$ mbar (nominal pressure).

shows that the reactions in Equations (2) and (3) are consecutive processes, as indicated in reference [5]. A value $k_1P_{\mathbf{I}}$ of 0.535 s^{-1} is obtained from the decay of $B_{ref}H^+$ by using the logarithmic form of Equation (6). Insertion of this value into Equations (7) and (8) leads to an average value of $k_2P_{\mathbf{I}}$ of 0.621 s^{-1}. The curves shown were constructed with these values. Formal uncertainties on k_1 and k_2 are estimated at approximately 10 and 17% respectively. In the case of the last three reference bases, only k_1 values can be determined. Uncertainties on these values can be estimated at 20–30%.

Computational methods: All calculations were performed by using the programs Gaussian 98 and 03.[17,18] The gas-phase basicity of **I** was calculated at the G3 level of theory[19] to ensure a reliable estimate of this magnitude. A cheaper approach was used to carry out the theoretical survey of the potential energy surface (PES) associated with the reaction in Equation (3) The geometries of all stationary points were optimized at the MP2/6-31G(d,p) level.[20]

In all cases, frequencies were calculated to ensure that the optimized structural parameters correspond to the equilibrium geometries in the case of the minima and to a first-order saddle point in the case of transition states.

The harmonic vibrational frequencies obtained at this level, corrected according to Radom scale factors,[21] were used to obtain the zero-point vi-

brational energies (ZPE), thermal correction to enthalpy (TCH) and entropies (S_m°).

In all cases, the intrinsic reaction coordinate (IRC)[22] path was constructed to check the energetic profile connecting each transition structure to the two associated minima of the proposed mechanism.

The MP2/6-31G(d,p) geometries were further refined at the MP2/6-311+G(d,p) level.[22] Finally, single-point energy calculations at the MP2/6-311+G(3df,2p) level were performed on these optimized structures.[23]

Electrophilic and nucleophilic Fukui functions[24] condensed to atoms were evaluated from single-point calculations performed on the ground-state structures of molecules as optimized at the same level of theory. Fukui functions were evaluated by using the coefficients of the frontier molecular orbitals (FMOs) involved in the reaction and the overlap matrix.

The global electrophilicity,[25] $\omega=(\mu^2/2\eta)$, is defined in terms of the chemical potential μ and the chemical hardness η.[26] Both quantities may be expressed in terms of the one-electron energies of the HOMO and LUMO molecular orbitals, ε_H and ε_L, as $\mu=(\varepsilon_H+\varepsilon_L)/2$ and $\eta=(\varepsilon_L-\varepsilon_H)$.[27]

Results and Discussion

Experimental results

We summarize in Table 1 the experimental values of k_1 and k_2 obtained as indicated above.

Table 1. Kinetic results pertaining to the protonation of **I**.

B_{ref}[a]	$GB[B_{ref}]$[a,b,c]	k_1[a,d]	ρ_{1norm}[a]	k_2[a,d]
H_2O	660.0	2.58 ± 0.26	1.00	0.87 ± 0.15
$CH_2(CN)_2$	694.1	1.55 ± 0.16	1.00	0.87 ± 0.15
CF_3CO_2nBu	733.8	1.30 ± 0.13	0.987	0.82 ± 0.14
n-C_4H_9CHO	764.8	1.05 ± 0.11	0.819	0.93 ± 0.16
HCO_2Et	768.4	0.842 ± 0.084	0.530	0.93 ± 0.16
HCO_2nPr	773.9	0.284 ± 0.028	0.198	0.86 ± 0.15
c-C_3H_5CN	777.5	0.189 ± 0.019	0.116	–[e]
CH_3COCH_3	784.8[f]	0.028 ± 0.006	0.0162	–[e]
CH_3CO_2Me	790.7	0.011 ± 0.003	0.0080	–[e]
Average k_2				0.87 ± 0.12[g]

[a] Defined in the text. [b] In kJ mol^{-1}. [c] From reference [9]. [d] In units of 10^{-9} cm^3 molecule^{-1} s^{-1}. [e] See text. [f] See ref. [28]. [g] Uncertainty taken as three standard deviations.

As expected, the rate of proton transfer from $B_{ref}H^+$ to **I** depends on $GB(B_{ref})$. On the other hand, k_2 is independent of $GB(B_{ref})$, a consequence of the fact that neither B_{ref} nor $B_{ref}H^+$ participate in the reaction in Equation (3). This is also consistent with the efficient thermalization of $\mathbf{I}H^+(g)$ prior to the reaction. On going from H_2O to HCO_2nPr, the ratio k_2/k_1 varies from 0.34 to 3.0. For bases stronger than the latter, the ratio is even larger. The protonation of **I** being the rate-determining step, no reliable k_2 values can then be extracted from these experimental data.

Even prior to a theoretical discussion of these processes, some important results can be obtained from the above.

*The gas-phase basicity of **I***: As mentioned earlier, GB(**I**) has been estimated to lie in the 764–781 kJ mol^{-1} range.[9] Using data from Table 1, it is possible to get a more precise value.

Consider the proton transfer between two bases, M and the reference base B_{ref}, respectively, Equation (10):

$$M + [B_{ref}H]^+ \rightarrow [MH]^+ + B_{ref} \qquad \Delta_r G_m^\circ(10) \tag{10}$$

Some years ago, Bouchoux and co-workers[29] drew attention to the fact that a correlation of the form of Equation (11) is observed between the experimental rate constant for this reaction, k, and the standard Gibbs energy change for reaction (10), $\Delta_r G_m^\circ(10)$.

$$\rho = \frac{k}{k_{coll}} = \frac{1}{1+\exp[(\Delta_r G_m^\circ(10) + \Delta_r G_a^\circ)/RT]} \tag{11}$$

In this expression, k_{coll} stands for the collision rate constant and $\Delta_r G_a^\circ$ is an apparent activation energy for Equation (10). This apparent activation energy is expected to be small and independent of the base B_{ref}. $\Delta_r G_m^\circ(10)$ is the difference between the gas-phase basicities of B_{ref} and M, $\Delta_r G_m^\circ(10) = GB(B_{ref}) - GB(M)$, and ρ is the "reaction efficiency" of the process.

Although the reaction in Equation (10) occurs at a low pressure and thus under single-collision conditions in which a temperature cannot be maintained by gas collisions, Bouchoux et al.[29] ascribed an effective temperature, T^*, to the collision complex, in a manner similar to that of Cooks[30] in the kinetic method. An effective temperature of about 550 K appears to describe adequately most experimental results. Bouchoux and co-workers parameterized Equation (11) in terms of parameters that depend only on the properties of M and not on the nature of the base and thus suggested the use of Equation (12) as a general expression for the study of the relationship between ρ and $\Delta_r G_m^\circ(10)$.

$$\rho = \frac{a}{1+\exp[b(\Delta_r G_m^\circ(9) + c)]} = \frac{a}{1+\exp[b(GB(B_{ref}) - GB(M) + c)]} \tag{12}$$

It was found that in general, the normalization factor a equals (0.90 ± 0.05) and $b=1/RT^*$ amounts to (3.8 ± 1.0) kJ^{-1} mol. $c=\Delta_r G_a^\circ$ is in the range of 2.5–6.0 kJ mol^{-1}.

Let us assume that GB(M) is unknown. Fitting the experimental ρ values for the proton transfer from series of protonated reference bases, $B_{ref}H^+$, to M through Equation (12) provides a means for its determination. This method has been quite successful, particularly when standard methods fail.[29b]

Figure 2 is a plot of the normalized value of $\rho_1 = k_1/k_{coll}$, namely ρ_{1norm} against $GB(B_{ref})$. For k_{coll}, the collision rate constant, we took a value of 2.66×10^{-9} cm^3 molecule^{-1} s^{-1}, as estimated by means of the ADO theory.[16] ρ_{1norm} is simply the ratio between the value of ρ_1 for any of the studied reactions and that for the fastest reaction (that with H_3O^+ in our case). $\rho_{1norm} = (k_1/k_{coll})/(k_1/k_{coll})_{max}$.

The constant k_1 for the reaction between H_3O^+ and **I** is $(2.58\pm0.26)\times10^{-9}$ cm^3 molecule^{-1} s^{-1}. This indicates that

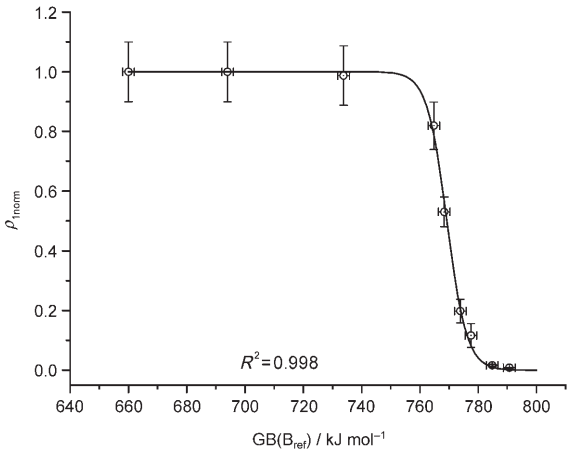

Figure 2. Thermokinetic plot for the reaction in Equation (2). Error bars for GB(B_{ref}) values and ρ_{1norm} are taken as 2 kJ mol^{-1} and as 10–30% (depending on B_{ref}, see Table 1), respectively.

proton transfer from protonated bases with GBs in the range of 660–734 kJ mol^{-1} takes place at essentially collision rate.

A referee has rightly observed that the determination of pressures is subject to considerable uncertainties and that the same applies to the estimation of k_{coll} by means of the ADO model (or even its improved versions). Here, these drawbacks are considerably reduced because ρ_{1norm} involves relative values. Furthermore, under these conditions, the comparison of the largest experimental rate constants and the computed k_{coll} is useful because it might reveal the existence of eventual complicating factors in the protonation process (none found here).

Fitting of ρ_{1norm} through Equation (11) yields values of (769.25 ± 0.23) kJ mol^{-1} and (0.293 ± 0.018) kJ^{-1} mol for GB(**I**) and b, respectively. The latter corresponds to an effective temperature of (410 ± 30) K.

2) *k_2 versus the collision rate constant*: ADO theory[16] provides an estimate of the collision rate constant for the process in Equation (3) of 1.54×10^{-9} cm^3 molecule^{-1} s^{-1}. The ratio k_2/k_{coll} thus equals (0.56 ± 0.14).

Computational treatment and discussion

GB(I): As mentioned above, we have carried out a study at the G3 level of species **I** and **I**H$^+$. The raw results are presented in Table S1 of the Supporting Information. They yield a value for GB(**I**) of 768.1 kJ mol^{-1}, a result agreeing within approximately 1 kJ mol^{-1} with the experimental value.

Ionization energies and electron affinities: Koopman's theorem allows the use of the HOMO and LUMO energies obtained in this study to estimate the ionization energy of **I**. We find a value of 9.5 eV, in reasonable agreement with the experimental vertical ionization energies reported in the literature (8.97–9.0 eV range).[9b,c] The estimated electron affinity (1.8 eV) is also quite consistent with the experimental value (1.75 eV).[9d]

Mechanism of the reaction in Equation (3): The fast reaction between **I** and **I**H$^+$ suggests the existence of an energetically favorable interaction between these two reagents prior to the bond-making–bond-breaking steps. Dispersion, ion-dipole and ion-induced dipole interactions are important contributors, but as we indicate below, more "specific" interactions probably exist:

Global and local electrophilicity analysis: In Table 2, the static global properties of neutral and protonated **I** are displayed. The electronic chemical potential[9] of **I** ($\mu = -0.1425$ hartree) is higher than that of **I**H$^+$ ($\mu = -0.3386$ hartree). As expected, the electron flow will take place from **I** to **I**H$^+$.

Table 2. Electronic chemical potential (μ), chemical hardness (η), and global electrophilicity (ω) of species **I** and **I**H$^+$.[a]

Species	HOMO	LUMO	μ	η	ω
I	−0.3505	0.0665	−0.1420	0.4170	0.66
IH$^+$	−0.5675	−0.1098	−0.3386	0.4578	3.41

[a] All values in hartree.

The electrophilicity values (ω) of **I** and **I**H$^+$, are 0.66 and 3.41 hartree, respectively. According to the absolute scale of electrophilicity[25] based on ω indexes, **I** and **I**H$^+$ may be classified as moderate and strong electrophiles, respectively.[31]

Analysis of **I** and **I**H$^+$ by means of Fukui functions[24] (Table 3) allows us to explain the regioselectivity of the polar process. The largest values of Fukui nucleophilic and electrophilic functions correspond to sulfur atoms S1(S2) ($f_k^- = 0.460$) and S3 ($f_k^+ = 0.605$), respectively (see Figure 4 for the numbering of atoms). Therefore, the latter will be the preferred site for a nucleophilic attack.

Table 3. Values of the nucleophilic, f_k^-, and electrophilic, f_k^+, Fukui functions for **I** and **I**H$^+$.

Species	Indexes	S1	S2
I	f_k^-	0.460	0.460
		S3	S4
IH$^+$	f_k^-	0.605	0.538

Energies: The calculated nuclear-plus-electronic energies, zero-point vibrational energies (ZPE), thermal corrections, and entropy values of the relevant species are summarized in Table S2 of the Supporting Information. Table 4 lists their relative nuclear-plus-electronic energies, ΔE_m, enthalpies, ΔH_m°, and Gibbs energies, ΔG_m°, relative to the separate reagents.

Table 4. MP2/6-311+G(3df,2p)//MP2/6-311+G(d,p) nuclear-plus-electronic energies (ΔE_m), enthalpies (ΔH_m°), entropies (ΔS_m°) and Gibbs energies (ΔG_m°) at 25 °C for all the stationary points relative to the separate reactants.[a]

Species	ΔE_m	ΔH_m°	$T\Delta S_m^\circ$	ΔG_m°
I+**IH**$^+$	0.0	0.0	0.0	0.0
R$_c$[b]	−68.20	−65.4	−34.2	−31.2
TS1	−49.20	−47.7	−36.3	−11.4
INT[c]	−79.79	−76.2	−33.3	−43.0
TS2	−60.75	−59.0	−38.0	−21.0
P$_c$[d]	−80.92	−77.5	−34.6	−42.9
II$^+$+**MeSH**	−42.76	−44.3	−1.6	−42.7

[a] All values in kJ mol^{-1}. [b] Reactive complex. [c] Intermediate. [d] Product complex.

The computed energetics profile of the reaction is represented in Figure 3. The structures of the various species involved are given in Figure 4.

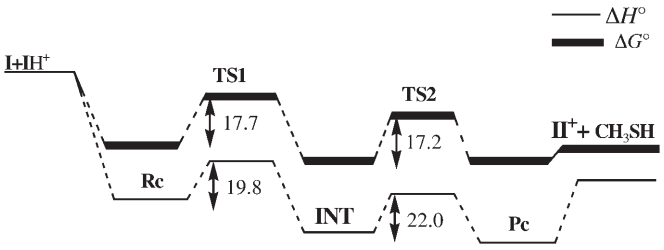

Figure 3. Enthalpy and Gibbs energy profiles for the reaction of **I** and **IH**$^+$ as computed at the MP2/6-311+G(d,p) level. Values in kJ mol^{-1}.

The reaction involves the initial formation of a reactive complex, **R**$_c$, 65.4 kJ mol^{-1} more stable than the separate reactants (in terms of ΔH_m°). This complex then overcomes the first transition state, **TS1**, leading to the intermediate **INT** and further evolves leading to a second intermediate, a product complex **P**$_c$, via a second transition state, **TS2.** **P**$_c$ is practically an adduct of **II**$^+$ and methyl mercaptan. Inspection of Figure 4 reveals that the first step corresponds to the nucleophilic attack of S2 of the neutral molecule on S3 of the protonated one to give the ionic reactive complex. The second step corresponds to the breaking of the S3–S4 bond and the formation of the S2–S3 bond. This step appears to be the key process of the reaction allowing the formation of **P**$_c$ through the formation of a new S–S bond. **P**$_c$ further decomposes leading to the departure of methanethiol and the formation of **II**$^+$. The feeble activation Gibbs energies associated with **TS1** and **TS2** favor the rapid evolution of the system. This reaction pattern is formally similar to that of cationic S_N2 reactions[32] and is consistent with the experimental kinetic results presented above. These results can be compared to those obtained in our studies involving the formal transfer of methyl groups in the gas phase.[10c] The activation Gibbs energies for these processes are much higher than those involved in the formal transfer of the thiomethyl group, relevant in this study.

The standard entropies for these species are strongly negative (in the range of −111.3 to −127.6 J mol^{-1} K^{-1}) with respect to the separate reagents, and they are responsible for the increase in the Gibbs energy of all the stationary points. The exception corresponds to the separate products in which it is only of −1.3 J mol^{-1} K^{-1}. Physically, the main contribution to these entropic effects originates in the loss of the translational entropy of the various systems with respect to the separate reagents. This entropy is recovered once the products separate.

At this point, we can look back at the fact that the rate constant k_2 is roughly half of the collision rate. The reactive complex **R**$_c$ is formed by the encounter of **I** and **IH**$^+$ oriented in such a way that they allow the reaction in Equation (3). However, this is not the only energetically favored encounter. **IH**$^+$ and **I** can also interact leading to a hydrogen-bonded complex (say between S4–H$^+$ and S1 or S2, Figure 4). A simple model, such as ADO, indicates that the collision frequencies for the two processes

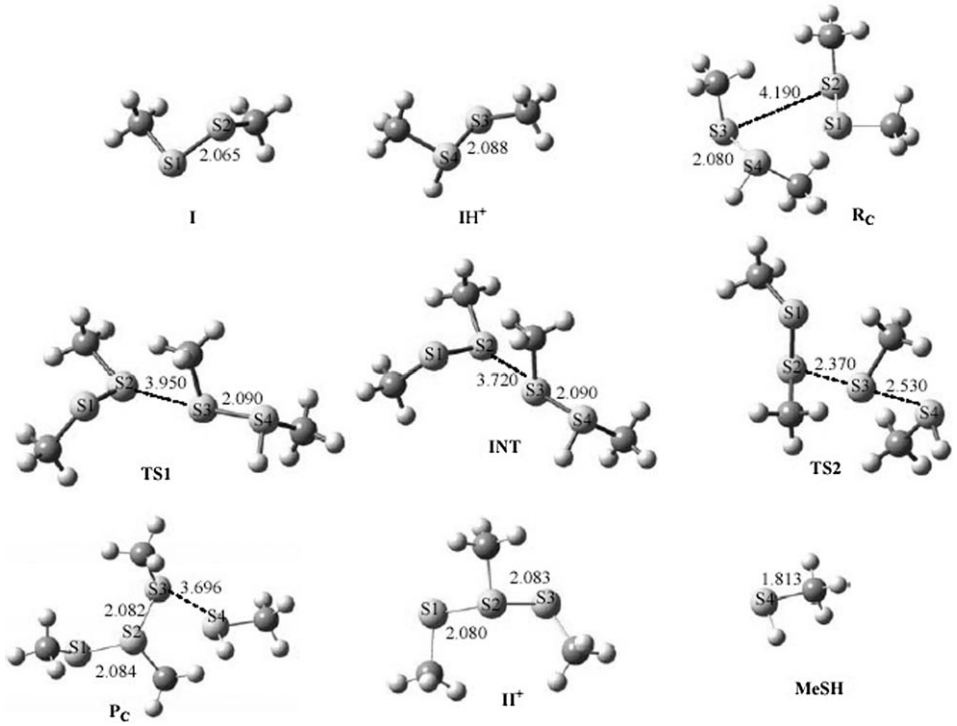

Figure 4. Structures optimized at the MP2/6-311+G(d,p) level of all species involved in the reaction pathway of **I** and **IH**$^+$. Bond lengths in Å.

Table 5. Evolution of the S–S interatomic distances (d, in Å), along the reaction path at the MP2/6-311+G(d,p) level. Charge density ($\rho(r)$) and energy density, $H(r)$ at the bond and ring critical points, bcp and rcp, respectively. All values in a.u. at the MP2/6-31+G(d,p)//MP2/6-311+G(d,p) level.

Species	$\mathbf{R_c}$	TS1	INT	TS2	$\mathbf{P_c}$	$\mathbf{II^+}$
$d_{(S1-S2)}$	2.07	2.07	2.07	2.08	2.08	2.06
$\rho_{(S1-S2)}$, $H_{(S1-S2)}$	0.1412, −0.0767	0.1417, −0.0771	0.1421, −0.0776	0.1397, −0.0753	0.1397, −0.0753	0.1404, −0.0765
$d_{(S2-S3)}$	4.17	3.95	3.72	2.37	2.08	2.08
$\rho_{(S2-S3)}$, $H_{(S2-S3)}$	–, –	0.0088, 0.0011	0.0054, 0.0009	0.0772, −0.0195	0.1399, −0.0758	0.1396, −0.0754
$d_{(S1-S3)}$	4.95	3.54	4.24	3.75	3.36	–
$\rho_{(S1-S3)}$, $H_{(S1-S3)}$	–, –	0.0077, 0.0010	–, –	–, –	–, –	–, –
$d_{(S3-S4)}$	2.08	2.09	2.09	2.53	3.70	–
$\rho_{(S3-S4)}$, $H_{(S3-S4)}$	0.1372, −0.0738	0.1345, −0.0718	0.1350, −0.0722	0.0563, −0.0091	–	–, –
$\rho_{(S1-S4)}$ $H_{(S1-S4)}$	0.0093, 0.0078					–, –
$\rho_{(S2-S4)}$, $H_{(S2-S4)}$	0.0089, 0.0011				0.0100, 0.0011	–, –
$\rho_{(S2\text{-}H\text{-}(C\text{-}S3))}$, $H_{(S2\text{-}H\text{-}(C\text{-}S3))}$	0.0077, 0.0011	0.0059, 0.0010	0.0046, 0.0075	–	0.0064[a], 0.0012[a]	–, –
$rcp_{(S1\text{-}S2\text{-}S3)}$, $H_{(S1\text{-}S2\text{-}S3)}$	–, –	0.0070, 0.0012	–	–	–	
$\rho_{(S1\text{-}H\text{-}(C\text{-}S3))}$, $H_{(S1\text{-}H\text{-}(C\text{-}S3))}$	0.0070[b], 0.0014[b]	0.0055, 0.0012	–	0.0144, 0.0010	–	–, –
$rcp_{(S1\text{-}H\text{-}C\text{-}S4)}$, $H_{(S1\text{-}H\text{-}C\text{-}S4)}$	0.0063[b], 0.0013[b]	0.0055, 0.0012	–, –	–, –	–, –	
$rcp_{(S2\text{-}H\text{-}C\text{-}S3)}$, $H_{(S2\text{-}H\text{-}C\text{-}S3)}$	0.0048[c], 0.0008[c]	0.0058, 0.0011	0.0043, 0.0007	–	–	
$rcp_{(S1\text{-}H\text{-}C\text{-}S3\text{-}S2)}$, $H_{(S1\text{-}H\text{-}C\text{-}S3\text{-}S2)}$	–, –	0.0053, 0.0011	–, –	0.0110, 0.0022	0.0052[d], 0.0011[d]	

[a] $\rho_{(S4\text{-}H\text{-}C\text{-}S3)}$. [b] $\rho_{(S1\text{-}H\text{-}C\text{-}S3)}$. [c] $rcp_{(S2\text{-}H\text{-}C\text{-}S3\text{-}S4)}$. [d] $rcp_{(S2\text{-}S4\text{-}H\text{-}C\text{-}S3)}$.

should be roughly the same. However, extensive exploration of the potential-energy surface of these systems carried out during the initial stages of this work, failed to show that they could lead to the reaction in Equation (3) at a low energetic cost. This explains why under the low working pressures, these complexes dissociate and approximately half of the total encounters do not lead to $\mathbf{II^+}$.

Geometries: The structures of the TSs and the intermediates corresponding to the reaction channel are displayed in Figure 4. The evolution of the S2–S3 and S3–S4 bond distances on going from the first adduct to the final intermediate are summarized in Table 5.

It can be seen that the S2–S3 distance varies from 4.17 Å, in $\mathbf{R_c}$ to 2.08 Å, in $\mathbf{P_c}$, indicating the S–S bond-making via **TS1** and **TS2**. At the same time, the distance S3–S4 varies from 2.08, in $\mathbf{R_c}$ to 3.70 Å in $\mathbf{P_c}$, indicating a bond-breaking via the same TSs. A closer look at the geometrical structures shows that TS2 is the main bond-making–bond-breaking process while TS1 constitutes an orientation transition state. Somewhat surprisingly, however, the standard Gibbs energies of activation involved in the formation of TS2 and TS1 are practically the same. An inspection of the topological analysis of the charge density of the species involved in the reaction pathway by means of the atoms in molecules (AIM) theory,[33] may offer some clues to understanding this question. The bond critical points (bcps) of the different stationary points along the PES are given in Table 5. Several conclusions can be drawn from this table. Firstly, the values of the charge density at the bond critical points exhibit a good correlation with the bond distances: the shorter the bond, the larger the ρ value. Secondly, as regards $\rho(r)$, further important points must be mentioned: 1) The fact that the ρ values are relatively low in the case of **TS1** indicates that it is effectively an orientation TS. 2) Among the ρ values corresponding to the making–breaking bonds, only those of **TS2** are relatively high. Therefore, $\rho(r)$s for the bonds S2−S3 and S3−S4 are roughly half of those for bonds S1−S2 (or S2−S3) in $\mathbf{II^+}$. 3) The existence of several bcps involving a hydrogen atom of a methyl group and the nearest sulfur atom. Here again, the largest value of ρ appears in the **TS2** structure. We have also located a ring critical point (rcp), nicely indicating the existence of an unconventional hydrogen bond stabilizing this transition state (Figure 5).

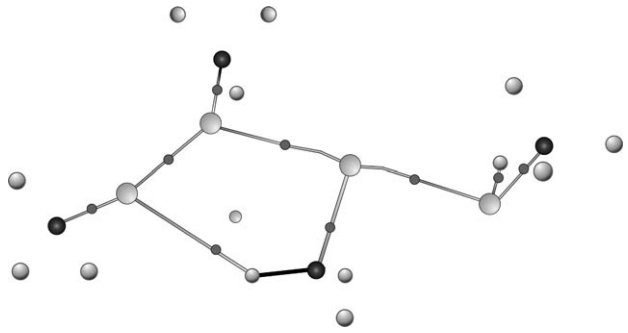

Figure 5. Molecular graph for **TS2**. Red dots are bcps. The yellow dot is the rcp pertaining to the five-membered structure. The C−H bonds are not represented, except in the case of S1−HCS3.

The ρ values at the bcp (0.014 a.u.) and at the rcp (0.011 a.u.) strongly suggest that the interaction is significant. Furthermore, the energy density, $H(r)$, which identifies regions of the space wherein the electronic charge is locally depleted ($H(r)>0$), as in hydrogen bonds or ionic bonds, or built up ($H(r)<0$)), as in covalent linkages, is positive at the S2−S3 bond of **TS1**, indicating that this interaction is weak and essentially electrostatic. Conversely, it is negative for the same linkage in TS2, indicating that already in the transition state the S2–S3 and S3–S4 interactions have a non-negligible covalent character. The overall molecular graph for **TS2** is presented in Figure 5. The combination of the S–S interactions and these hydrogen bonds efficiently stabilizes **TS2**.

Equilibria: Further conclusions can be extracted from the above:

1) The low activation barriers separating species $\mathbf{R_c}$, **INT** and $\mathbf{P_c}$ should allow their fast interconversion. More precisely, we might consider the reactions in Equations (13)

$$\mathbf{R_c} \rightarrow \mathbf{INT} \qquad \Delta_r G_m^\circ(13) K_p(13) \tag{13}$$

and (14):

$$\mathbf{INT} \rightarrow \mathbf{P_c} \qquad \Delta_r G_m^\circ(14) K_p(14) \tag{14}$$

From the data given in Table 4, we obtain $\Delta_r G_m^\circ(13) = -11.7$ and $\Delta_r G_m^\circ(14) = -11.6\ \mathrm{kJ\,mol^{-1}}$. Then, $K_p(13) \approx K_p(14) = 1.1 \times 10^2$. The equilibrium in Equation (15) is pressure dependent:

$$\mathbf{P_c} \rightarrow \mathbf{II}^+ + \mathrm{MeSH} \qquad \Delta_r G_m^\circ(15)\ K_p(15) \tag{15}$$

For this process, $\Delta_r G_m^\circ(15) = -3.1\ \mathrm{kJ\,mol^{-1}}$ and $K_p(15) = 3.5$.[34] It is clear, therefore, that under pressures of the order of 1 atm or higher, one could observe an equilibrating mixture of species $\mathbf{II}^+$, MeSH, $\mathbf{P_c}$, and **INT**. In our experiments, this is not the case, simply because the very low working pressure shifts the reaction in Equation (15) to the right.

2) Going back to the global and local electrophilicity analysis, we see that the formation of $\mathbf{R_c}$ and its evolution towards **INT** is driven by the nucleophilic attack of a S atom of **I** on the proton-activated S–S bond of $\mathbf{IH}^+$. Conversely, the formation of $\mathbf{P_c}$ as well as that of **INT** can be viewed as a consequence of a nucleophilic attack of the sulfur atom of MeSH on an activated S–S bond of $\mathbf{II}^+$. In both cases, S–S bonds are activated by an electron-attracting center. This is closely related to the reversible binding of PPIs to gastric (H^+,K^+)-ATPase indicated above.

Theso-called chalcogen–chalcogen interaction has recently received considerable attention.[35] In the particular case of sulfur derivatives, it has been shown that dispersive and inductive interactions between substituted chalcogen atoms are important. So are the hydrogen-bonding interactions C–H···S.[35a] Quite recently,[35b] a very high-level computational study on the interaction between species Me–X–Z (X being the chalcogen and Z, Me, or a stronger electron-withdrawing substituent) and XMe_2 has fully confirmed these findings and further validated on a semiquantitative basis the one-electron picture of a stabilizing interaction between the lone pair of the donor and the chalcogen–carbon σ* orbital. The quantitative importance of this interaction increases with the electron-withdrawing ability of Z. Our results show that all these factors are involved in the stabilization of TS2.

Conclusion

The experimental study of the gas-phase protonation of dimethyldisulfide has provided, we believe for the first time, a rather precise value of its gas-phase basicity (the accuracy is possibly lower). This value agrees to within $1\ \mathrm{kJ\,mol^{-1}}$ with the results of G3 calculations.

Also obtained for the first time was the reaction rate constant for the bimolecular reaction between neutral and protonated dimethyldisulfide to yield methanethiol and dimethyldithiosulfonium ion. This constant is of the order of magnitude of the collision limit. A computational mechanistic study based on the energetic profile of the reaction, completed with Fukui's and Bader's treatments of the reactants and transition states fully rationalizes the regioselectivity of the reaction as well as the existence of a shallow, flat Gibbs energy surface for the reaction. The mechanistic relevance of the chalcogen–chalcogen interaction and the C–H···S bonds has been demonstrated.

Acknowledgements

This work was supported by grants BQU2003-05827 and BQU2003-00894 of the Spanish DGIYT, and by the Project MADRISOLAR. Ref.: S-0505/PPQ/0225 of the Comunidad Autónoma de Madrid. Support from a joint CNRST (Morocco)–CSIC (Spain) project is also gratefully acknowledged. Valuable comments by the referees are most appreciated.

[1] *Sulfur in Proteins* (Eds.: B. Reinhold, R. E. Benesch, P. D. Boyer, I. M. Klotz, W. R. Middlebrook, A. Szent-Györgi, R. D. Schwarz), Academic Press, New York, **1959**.
[2] a) A. Fehrst, *Structure and Mechanism in Protein Science*, W. H. Freeman, New York, **2002**, pp. 534–535, 574–575; b) J. Clayden, N. Greeves, P. Wothers, *Organic Chemistry*, Oxford University Press, New York, **2001**. Chapter 49, pp. 1354–1355.
[3] S. F. Betz, *Protein Sci.* **1993**, *2*, 1551–1558.
[4] J. M. Shin, Y. M. Cho, G. Sachs, *J. Am. Chem. Soc.* **2004**, *126*, 7800–7811.
[5] P. J. Lawrence, *Biochemistry* **1969**, *8*, 1271–1278.
[6] a) A. G. Marshall, C. L. Hendrickson, *Int. J. Mass Spectrom.* **2002**, *215*, 59–75; b) J.-F. Gal, P.-C. Maria, E. W. Raczynska, *J. Mass. Spectrom.* **2001**, *36*, 699–716; c) J.-L. M. Abboud, R. Notario in *Energetics of Stable Molecules and Reactive Intermediates* (Ed.: M. E. Minas da Piedade), NATO Science Series C, 535, Kluwer, Dordrecht, **1999**, pp. 281–302; d) A. G. Marshall, C. L. Hendrickson, G. S. Jackson, *Mass Spectrom. Rev.* **1998**, *17*, 1–35; e) F. H. Laukien, M. Allemann, P. Bischopfberger, P. Grossmann, P. Kellerhals, P. Kopfel in *Fourier Transform Mass Spectrometry. Evolution, Innovation and Applications* (Ed.: M. V. Buchanan), ACS Symp. Ser., 359, American Chemical Society, Washington, DC, **1987**, Chapter 5.
[7] J. K. Kim, J. Bonicamp, M. C. Caserio, *J. Org. Chem.* **1981**, *46*, 4230–4236.
[8] The gas-phase basicity of a base B, GB(B), is defined[9a] as the standard Gibbs energy change for reaction, Equation (16):
$BH^+(g) \rightarrow B(g) + H^+(g) \quad GB(B) = \Delta_r G_m^\circ$ (16)
[9] a) E. P. L. Hunter, S. Lias, *J. Phys. Chem. Ref. Data* **1998**, *27*, 413–656; b) "*Neutral Chemical Data*", S. G. Lias, J. E. Bartmess, J. F. Liebman, J. L. Holmes, R. D. Levine, W. G. Mallard in *NIST Chemistry Webbok*, *NIST Standard Reference Database Number 69* (Eds.: P. J. Linstrom, W. G. Mallard), June **2005**, National Institute of Science and Technology, MD, 20899 (http://webbook.nist.gov); c) "*Ion Energetics Data*", S. G. Lias, R. D. Levin, S. A. Kafafy in

NIST Chemistry Webbok, *NIST Standard Reference Database Number 69* (Eds.: P. J. Linstrom, W. G. Mallard), June **2005**, National Institute of Science and Technology, MD, 20899 (http://webbook.nist.gov); d) S. Carles, F. Lecomte, J. P. Schermann, C. Desfrançois, S. Xiu, J. M. Nilles, K. H. Bowen, J. Howe, *J. Phys. Chem. A* **2001**, *105*, 5622–5626.

[10] a) J.-L. M. Abboud, I. A. Koppel, I. Alkorta, E. W. Della, P. Müller, J. Z. Dávalos, P. Burk, I. Koppel, V. Pihl, E. Quintanilla, *Angew. Chem. Int. Ed.* **2003**, *42*, 2281–2285; b) E. Quintanilla, J. Z. Dávalos, J.-L. M. Abboud, M. Alcamí, M. P. Cabildo, R. M. Claramunt, J. Elguero, O. Mó, M. Yáñez, *Chem. Eur. J.* **2005**, *11*, 1826–1832; c) J. Z. Dávalos, R. Herrero, E. Quintanilla, P. Jiménez, J.-F. Gal, P.-C. Maria, J.-L. M. Abboud, *Chem. Eur. J.* **2006**, *12*, 5505–5513.

[11] J. E. Bartmess, R. M. Giorgiadis, *Vacuum* **1983**, *33*, 149–153.

[12] K. J. Miller, *J. Am. Chem. Soc.* **1990**, *112*, 8533–8542.

[13] For example see: I. N. Levine, *Physical Chemistry*, McGraw Hill, New York, 5th ed., **2002**, pp. 537–538.

[14] T. V. Frigden, J. D. Keller, T. B. MacMahon, *J. Phys. Chem. A* **2001**, *105*, 3816–3824.

[15] This is the collision rate constant k_{coll} for the reaction (9), calculated according to the ADO model.[16]

[16] T. Su, M. T. Bowers in *Gas Phase Ion Chemistry, Vol 1.* (Ed.: M. T. Bowers), Academic Press, New York, **1979**, Chapter 3, 84–95, and references therein.

[17] Gaussian 98 (Revision A.7), M. J. Frisch, G. W. Trucks, H. B. Schlegel, G. E. Scuseria, M. A. Robb, J. R. Cheeseman, V. G. Zakrzewski, J. A. Montgomery, Jr., R. E. Stratmann, J. C. Burant, S. Dapprich, J. M. Millam, A. D. Daniels, K. N. Kudin, M. C. Strain, O. Farkas, J. Tomasi, V. Barone, M. Cossi, R. Cammi, B. Mennucci, C. Pomelli, C. Adamo, S. Clifford, J. Ochterski, G. A. Petersson, P. Y. Ayala, Q. Cui, K. Morokuma, D. K. Malick, A. D. Rabuck, K. Raghavachari, J. B. Foresman, J. Cioslowski, J. V. Ortiz, B. B. Stefanov, G. Liu, A. Liashenko, P. Piskorz, I. Komaromi, R. Gomperts, R. L. Martin, D. J. Fox, T. Keith, M. A. Al-Laham, C. Y. Peng, A. Nanayakkara, C. Gonzalez, M. Challacombe, P. M. W. Gill, B. G. Johnson, W. Chen, M. W. Wong, J. L. Andres, M. Head-Gordon, E. S. Replogle, J. A. Pople, Gaussian, Inc., Pittsburgh, PA, **1998**.

[18] Gaussian 03 (Revision B.05), M. J. Frisch, G. W. Trucks, H. B. Schlegel, G. E. Scuseria, M. A. Robb, J. R. Cheeseman, J. A. Montgomery, Jr., T. Vreven, K. N. Kudin, J. C. Burant, J. M. Millam, S. S. Iyengar, J. Tomasi, V. Barone, B. Mennucci, M. Cossi, G. Scalmani, N. Rega, G. A. Petersson, H. Nakatsuji, M. Hada, M. Ehara, K. Toyota, R. Fukuda, J. Hasegawa, M. Ishida, T. Nakajima, Y. Honda, O. Kitao, H. Nakai, M. Klene, X. Li, J. E. Knox, H. P. Hratchian, J. B. Cross, V. Bakken, C. Adamo, J. Jaramillo, R. Gomperts, R. E. Stratmann, O. Yazyev, A. J. Austin, R. Cammi, C. Pomelli, J. W. Ochterski, P. Y. Ayala, K. Morokuma, G. A. Voth, P. Salvador, J. J. Dannenberg, V. G. Zakrzewski, S. Dapprich, A. D. Daniels, M. C. Strain, O. Farkas, D. K. Malick, A. D. Rabuck, K. Raghavachari, J. B. Foresman, J. V. Ortiz, Q. Cui, A. G. Baboul, S. Clifford, J. Cioslowski, B. B. Stefanov, G. Liu, A. Liashenko, P. Piskorz, I. Komaromi, R. L. Martin, D. J. Fox, T. Keith, M. A. Al-Laham, C. Y. Peng, A. Nanayakkara, M. Challacombe, P. M. W. Gill, B. Johnson, W. Chen, M. W. Wong, C. Gonzalez, J. A. Pople, Gaussian, Inc., Wallingford CT, **2004**.

[19] L. A. Curtiss, K. Raghavachari, P. C. Redfern, V. Rassolov, J. A. Pople, *J. Chem. Phys.* **1998**, *109*, 7764–7776.

[20] M. Frisch, J. A. Pople, J. A. Binkley, *J. Chem. Phys.* **1984**, *80*, 3265–3269.

[21] A. P. Scott, L. Radom, *J. Phys. Chem.* **1996**, *100*, 16502–16513.

[22] W. J. Hehre, L. Radom, P. v. R. Schleyer, J. A. Pople, *Ab Initio Molecular Orbital Theory*, Wiley-Interscience, New York, **1986**.

[23] R. Krishnan, J. S. Binkley, R. Seeger, J. A. Pople, *J. Chem. Phys.* **1980**, *72*, 650–654.

[24] K. Fukui, *J. Phys. Chem.* **1970**, *74*, 4161–4163.

[25] R. G. Parr, W. Yang, *J. Am. Chem. Soc.* **1984**, *106*, 4049–4050.

[26] R. G. Parr, L. v. Szentpaly, S. Liu, *J. Am. Chem. Soc.* **1999**, *121*, 1922–1924.

[27] R. G. Parr, R. G. Pearson, *J. Am. Chem. Soc.* **1983**, *105*, 7512–7516.

[28] Average of the experimental data reported in reference [9]

[29] a) G. Bouchoux, J. Y. Salpin, D. Leblanc, *Int. J. Mass Spectrom. Ion Processes* **1996**, *153*, 37–48; b) for example see: G. Bouchoux, J. Y. Salpin, *J. Am. Chem. Soc.* **1996**, *118*, 6516–6517.

[30] a) R. G. Cooks, T. L. Kruger, *J. Am. Chem. Soc.* **1977**, *99*, 1279–1281; b) R. G. Cooks, J. S. Patrick, T. Kotiaho, S. A. McLuckey, *Mass Spectrom. Rev.* **1994**, *13*, 287–339; c) R. G. Cooks, P. S. H. Wong, *Acc. Chem. Res.* **1998**, *31*, 379–386.

[31] P. Pérez, L. R. Domingo, M. J. Aurell, R. Contreras, *Tetrahedron* **2003**, *59*, 3117–3125.

[32] a) D. K. Sen Sharma, P. Kebarle, *J. Am. Chem. Soc.*, **1982**, *104*, 19; b) M. J. Pellerite, J. I. Brauman, *J. Am. Chem. Soc.* **1980**, *102*, 5993–5999; c) G. Caldwell, T. F. Magnera, P. Kebarle, *J. Am. Chem. Soc.* **1984**, *106*, 959–966.

[33] R. F. W. Bader, *Atoms in Molecules. A Quantum Theory*, Clarendon Press, Oxford, **1990**.

[34] This, as all other K_p values, is dimensionless.

[35] For example see: a) P. Sanz, O. Mó, M. Yáñez, *J. Phys. Chem. A* **2002**, *106*. 4661–4668; b) C. Bleiholder, D. B. Werz, H. Köppel, R. Gleiter, *J. Am. Chem. Soc.* **2006**, *128*, 2666–2674, and references therein.

Received: May 25, 2006
Published online: November 24, 2006

